Table 1 POWER BUDGET FOR BOTH CHANNELS

	$1 \cdot 3\,\mu m$ system		$1 \cdot 5\,\mu m$ system
Launch power	−2·4 dBm		−3·2 dBm
Power after 1st coupler	−5·9 dBm		−7·8 dBm
1st link loss	32·5 dB		9·8 dB
Power into 1st demux	−38·4 dBm		−17·6 dBm
Power into 1st receiver	−39·9 dBm	Power into EDFA	−19·1 dBm
Effective regenerator gain	35·6 dB	Amplifier gain	15·6 dB
Relaunch power	−4·3 dBm	Power out of EDFA	−3·5 dBm
Power after coupler	−7·7 dBm		−6·9 dBm
2nd link loss	26·1 dB		20·6 dB
Power into 2nd demux	−33·8 dBm		−27·5 dBm
Final received power	−35·0 dBm		−29·0 dBm
Receiver sensitivity	−36·5 dBm		−29·2 dBm
System penalty	1·5 dB		0·2 dB

system could potentially use 58·6 dB of fibre attenuation, the $1 \cdot 5\,\mu m$ system has only 30·4 dB available. This was due partly to the poor $1 \cdot 5\,\mu m$ receiver sensitivity, and also because the amplifier gain was 20 dB lower than the effective regenerator gain. Signal to noise ratio considerations require the signal input to the amplifier to be fairly large, thus limiting the first span loss and also driving the amplifier to some extent into saturation thus accounting for the relatively small amplifier gain. As each system would in practice use the same fibre, the extra loss of the $1 \cdot 3\,\mu m$ window (0·34 dB/km) compared to the $1 \cdot 5\,\mu m$ system (0·22 dB/km) reduces the 28·2 dB discrepancy to only 7·5 dB. The penalty incurred by the $1 \cdot 3\,\mu m$ system was due to imperfect isolation of the wavelength selective filters. The use of cascaded, fused, tapered couplers with net isolations greater than 45 dB would eliminate this penalty, although the device would need to maintain this isolation over a broad wavelength range. The two 50 : 50 couplers, while providing a broadband wavelength split, nevertheless remove at least 6 dB from the power budget of both channels, and these could also be replaced by wavelength sensitive couplers having an excess loss of $< 0 \cdot 5$ dB.

Conclusions: A technique for opening up the $1 \cdot 5\,\mu m$ transmission window in established $1 \cdot 3\,\mu m$ regenerated networks has been proposed. The method, which uses an optical amplifier for the $1 \cdot 5\,\mu m$ link, has been successfully demonstrated in laboratory experiments. Although the presence of regenerators limits the $1 \cdot 3\,\mu m$ system to a fixed data format, the use of wideband optical amplifiers in the $1 \cdot 5\,\mu m$ path allows for a much greater flexibility in the upgrade channel.

The series of measurements carried out on the demonstration system showed that the inclusion of the $1 \cdot 5\,\mu m$ channel resulted in a degradation of only 1·5 dB in the $1 \cdot 3\,\mu m$ channel performance. Allowing for the losses of four couplers, overall reduction in usable power budget for the complete system could be less than 5 dB. The performance of the $1 \cdot 5\,\mu m$ system could be expected to match that of the $1 \cdot 3\,\mu m$ system if, along with an improved receiver, an amplifier with higher saturated output power was used. The extra fibre loss at $1 \cdot 3\,\mu m$ will in part balance the lower gain of the $1 \cdot 5\,\mu m$ channel.

J. M. BOGGIS
A. LORD
W. A. STALLARD
P. COCHRANE

British Telecom Research Laboratories
Martlesham Heath
Ipswich IP5 7RE, UK

25th October 1990

References

1 BRYANT, E. G., *et al.*: 'A 1·2 Gbit/s optical FSK field trial demonstration', *British Telecom Technology Journal*, 1990, **8**, (2), pp. 18–26
2 BRYANT, E. G., *et al.*: 'Two-way transmission at 2·488 Gbit/s over a 132 km operational submerged cable using erbium-doped fibre power amplifiers', *Electron. Lett.*, 1990, **26**, (17), pp. 1355–1356
3 HUNWICKS, A. R., *et al.*: 'Duplex-diplex optical transmission in the 1300 nm and 1500 nm fibre windows: an installed system', *Electron. Lett.*, 1987, **23**, (10), pp. 542–544
4 LORD, A., *et al.*: 'A four channel WDM submarine field trial'. Proc. ECOC, Gothenburg, Sweden, September 1989, pp. 466–469
5 STEELE, R. C., *et al.*: 'Field trial of 565 Mbit/s DPSK heterodyne system over 108 km'. Proc. ECOC, post-deadline papers, Brighton, September 1988, pp. 61–64
6 CREANER, M. J., *et al.*: 'Field demonstration of coherent transmission system with diode-pumped erbium doped fibre amplifiers', *Electron. Lett.*, 1990, **26**, (7), pp. 442–444
7 BROOKS, R. M., *et al.*: 'A highly integrated 565 optical fibre system', *Br. Telecom Tech. J.*, 1986, **4**, (4), pp. 28–40
8 LORD, A., *et al.*: 'Comparison of WDM coupler technologies for use in erbium doped fibre amplifier systems', *Electron. Lett.*, 1990, **26**, (13), pp. 900–901

ALL-OPTICAL INVERTER WITH ONE PICOJOULE SWITCHING ENERGY

Indexing terms: Optical fibres, Inverters, Logic devices

An ultrafast inverter based on soliton dragging in optical fibres with a switching energy of only 1 pJ, which is the lowest switching energy of any all-optical device, is demonstrated. The inverter consists of a 30 m length of moderately birefringent fibre followed by a 2 km length of a polarisation maintaining fibre. The switching energy is lowered by separating the soliton dragging mechanisms in two different fibres and optimising the parameters in a time domain chirp switch that is based on time shift keying logic.

Recently all-optical, cascadable, soliton dragging logic gates with gain have been demonstrated that switch at an energy of 5·8 pJ.[1] The digital logic is based on time shift keying in which a logical one corresponds to a control pulse that arrives within a clock window and a logical zero to either a control pulse outside of the clock window or no pulse at all. Because of power supply limitations, the key issue for ultrafast gates is how to lower the switching energy. By separating the soliton dragging mechanisms in two different fibres and optimising each section individually, we reduce the switching energy for an inverter down to 1 pJ. Although a 2 km long logic gate may not be practical, our purpose here is to show that even in fused silica fibres an all-optical gate can fundamentally approach the 1 pJ switching energy level, which then makes potential applications feasible.

We consider a time domain chirp switch architecture* that consists of a nonlinear chirper followed by a soliton dispersive delay line and has two orthogonally polarised inputs (signal and control pulses). In the absence of a signal pulse, the control pulse propagates through both sections and arrives at the output within the clock window. Adding the temporally coincident signal chirps or frequency shifts the control pulse, and the shift transforms into a time change ΔT after propagating in the dispersive second section. In our soliton dragging experiments the nonlinear chirper corresponds to a two

* ISLAM, M. N., CHEN, C. J., and SOCCOLICH, C. E.: 'All-optical time-domain chirp switches', submitted to *Optics Letters*

walk-off length of moderately birefringent fibre and the soliton dispersive delay line corresponds to a long polarisation maintaining fibre (see insert to Fig. 1). For this two-fibre soliton determined by requiring sufficient chirp to shift the control pulse, and the control energy is determined by requiring the control to be a fundamental soliton in the second fibre.

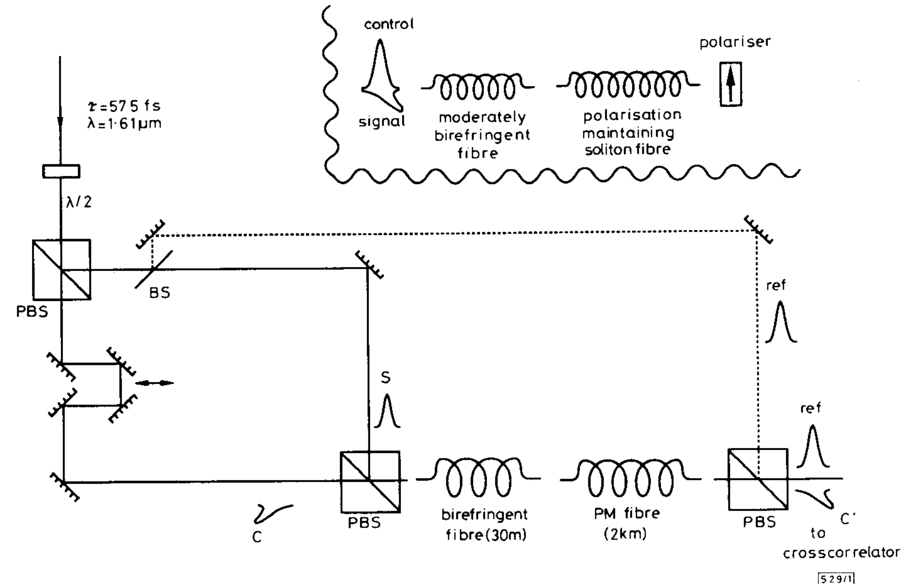

Fig. 1 *Experimental apparatus for testing one picojoule switching energy soliton dragging inverter*

PBS = polarising beam splitter
BS = beam splitter
PM = polarisation maintaining
The insert shows a schematic of the soliton dragging time domain chirp switch

dragging case we find that the switching energy E_s is proportional to* $E_s \propto (\Delta T/\tau) \cdot \tau^2 \cdot \Delta n_1/(L_2 \cdot D_2)$, where τ is the pulse width, Δn_1 is the birefringence in the first fibre, and L_2 and D_2 are the length and group velocity dispersion in the second fibre. Thus, the birefringence of the first fibre and the dispersion in the second fibre are the crucial fibre parameters. Assuming that $\Delta T/\tau$ is a constant, two ways of reducing E_s are to lower Δn_1 and to increase the length (or number of soliton periods) of the second fibre. We cannot reduce the pulse width below ~500 fs because of soliton self-frequency shift (SSFS)[1,2] effects, and we hesitate to increase the dispersion in the second fibre because this increases the soliton energy and, consequently, the control energy.

The experimental apparatus for testing the inverter is shown in Fig. 1. A passively modelocked colour centre laser supplies $\tau \sim 575$ fs pulses near 1·61 μm. The input stage separates the control and signal pulses, permits them to be independently varied, and then recombines them overlapped in time. For the 1 pJ inverter we use 30 m of moderately birefringent fibre followed by a 2 km length of polarisation maintaining fibre. The birefringence in the first fibre is $\Delta n_1 \sim 10^{-5}$ and the polarisation extinction ratio is ~30 : 1. The polarisation maintaining fibre has a dispersion of $D_2 = 12{\cdot}3$ ps/(nm km) at 1·61 μm and an extinction ratio of ~7 : 1. A polarisation maintaining fibre is required in the second section to avoid nonlinear polarisation rotation effects,[3] and because of the high birefringence there is little interaction between the signal and control pulses in the second fibre. Furthermore, the core size and, consequently, the soliton energy of the second fibre is larger than that for the first fibre. Finally, the output control pulse is combined with a reference pulse, and the two are sent to a crosscorrelator.

The correlation of the control output with the reference pulse is shown in Fig. 2A. The rectangle outlines the clock window, and we see that adding the signal shifts the control pulse out of this window. The signal energy in the first fibre is 1 pJ and the control energy out of the second fibre is 28 pJ, which corresponds to a fanout of 28. The signal energy is

Despite the shift in peak by ~4 ps, the contrast within the clock window is limited by the broadening of the crosscorrelation. The crosscorrelation broadens because of jitter during the 9·7 μs latency through the 2 km fibre and because the control energy in the second fibre is lower than an $N = 1$ soliton. For example, we estimate the control power to be about 0·45 times the $N = 1$ soliton power P_1; although this is still a fundamental soliton, the width adjusts to compensate for the lower power. From the autocorrelation of the control output pulse in Fig. 2B we find that the pulse broadens to 1·3 ps (autocorrelation width is $\sqrt{(2)}$ times the pulse width), which is 2·3 times the input pulse width.

We purposely stay below the $N = 1$ soliton energy in the second fibre to avoid SSFS. Frequency shifting deleteriously affects the switch because it translates amplitude jitter into timing jitter and because the gate is not cascadable if the frequency shifts down. We plot in Fig. 3 the measured spectral shift $\delta\nu$ normalised to the original spectra width $\Delta\nu_0$ against the control power P_c/P_1 for propagation through only the second fibre. The spectral shift has an almost diode-like characteristic with the knee around $P_c/P_1 \sim 0{\cdot}5$. This behaviour comes from the strong dependence of SSFS on pulse width ($\delta\nu \propto \tau^{-4}$), and the output pulse width against control power is also plotted in Fig. 3.

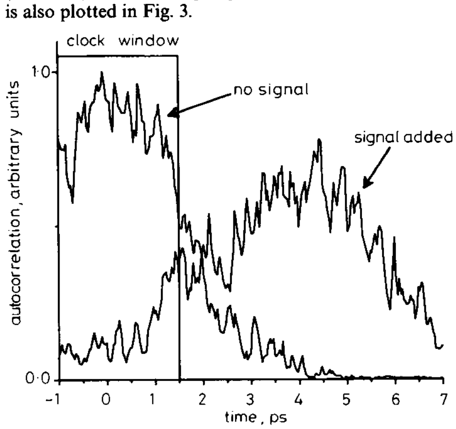

Fig. 2A *Crosscorrelation of control pulse out with reference pulse*

Although broader pulses reduce the soliton self-frequency shift, we still prefer to have $\tau_{out}/\tau_{in} \sim 1$ because of cascadability and for improved contrast in the crosscorrelation.

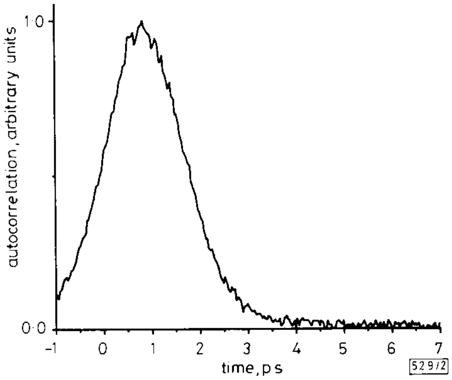

Fig. 2B *Autocorrelation of control pulse emerging from inverter*

Despite the adiabatic broadening, the control pulse can be recompressed at the output by introducing a third fibre. From perturbation theory we know that the asymptotic value of the soliton is $(1 + 2a)$ sech $[(1 + 2a)t]$ when we start with an input electric field $(1 + a)$ sech (t). We can recompress an $a < 0$ pulse either by amplifying the output and then coupling into another fibre or by going straight into another fibre with a lower soliton energy. If the output from the long fibre enters another fibre with normalised amplitude $(1 + G)(1 + 2a)$, where $(1 + 2G) = (1 + 2a)^{-1}$, then the pulse shrinks back to its original pulse width in a few soliton periods. For example, we have done computer simulations for $-0{\cdot}25 < a < -0{\cdot}2$ and find that τ_{out}/τ_{in} returns to 1 within 2 to 2·5 soliton periods.

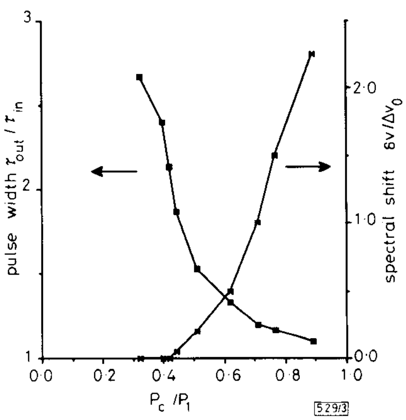

Fig. 3 *Spectral shift $\delta\nu$ normalised to the original spectral width $\Delta\nu_0$ (right axis) and broadening of control pulse τ_{out}/τ_{in} (left axis) in 2 km long polarisation maintaining fibre as function of input power P_c/P_1*

In summary, we demonstrate a soliton dragging inverter based on time shift keying with a switching energy of only 1 pJ and a control energy of 28 pJ. Although the pulse width is broadened to avoid SSFS in the 2 km fibre, the output can be recompressed in a short segment of another fibre.

Acknowledgment: C.-J. Chen's work is supported by the US Department of Energy.

7th November 1990

M. N. ISLAM
C. E. SOCCOLICH
C.-J. CHEN
K. S. KIM
J. R. SIMPSON
U. C. PAEK

AT&T Bell Laboratories
Holmdel, New Jersey 07733, USA

References

1 ISLAM, M. N., SOCCOLICH, C. E., and MILLER, D. A. B.: 'Low-energy ultrafast fiber soliton logic gates', *Opt. Lett.*, 1990, **15**, pp. 909–911
2 GORDON, J. P.: 'Theory of the soliton self-frequency shift', *Opt. Lett.*, 1986, **11**, pp. 662–664
3 ISLAM, M. N., SOCCOLICH, C. E., GORDON, J. P., and PAEK, U. C.: 'Soliton intensity-dependent polarization rotation', *Opt. Lett.*, 1990, **15**, pp. 21–23

MONOLITHIC InP-BASED GRATING SPECTROMETER FOR WAVELENGTH-DIVISION MULTIPLEXED SYSTEMS AT 1·5 μm

Indexing terms: Spectrometry, Optical communication

A monolithic InP-based grating spectrometer for use in wavelength-division multiplexed systems at 1·5 μm is reported. The spectrometer uses a single etched reflective focusing diffraction grating and resolves >50 channels at 1 nm spacing with a ~0·3 nm channel width and at least 19 dB channel isolation. Operation is essentially of the state of the input polarisation.

Introduction: Wavelength-division multiplexed (WDM) systems are currently being investigated for optical data transmission in telecommunications and computer local area networks.[1] Compact hybrid demultiplexers have been reported for use in such systems.[2] However, integration offers the advantages of small size, reliability, and a low unit cost, and implementation in semiconductor material allows monolithic integration with sources[3] and detectors.[4]

An integrated demultiplexer fabricated in planar InP/InGaAsP waveguide material employing a high order transmission grating and concave mirrors has been reported.[5] Recently, a reflection grating demultiplexer demonstrating 20 channels with a 4 nm wavelength spacing was described.[6] We report a monolithic InP-based single grating spectrometer which resolves >50 wavelength channels at a 1 nm spacing with 0·3 nm channel width and better than 19 dB channel isolation. The spectrometer may be operated so that it is completely polarisation-insensitive. This is the best spectral performance reported to-date for a multichannel semiconductor-based wavelength demultiplexer.

Design and fabrication: The integrated spectrometer was formed in a InP/InGaAsP/InP planar waveguide.[7] Based on a Rowland circle construction,[8] it used a single vertical-walled reflection focusing diffraction grating, implemented in a Littrow-type configuration, to perform the wavelength dispersion. Identical, equally spaced, single moded ridge waveguides formed the input and output ports. A schematic diagram of the device is shown in Fig. 1.

The spectrometer was designed to operate around 1·5 μm, with a channel spacing of 1 nm. The grating had a *d*-spacing of 5·1 μm, operated in 18th order, and was blazed for retroreflective diffraction at 1·51 μm. The waveguides had 9 μm wide ridges and were spaced at 20 μm. The optical body of the spectrometer was ~11 mm × 1·6 mm. A double heterostructure guide, InP/1·1 μm InGaAsP (λ_{gap} = 1·0 μm)/0·6 μm

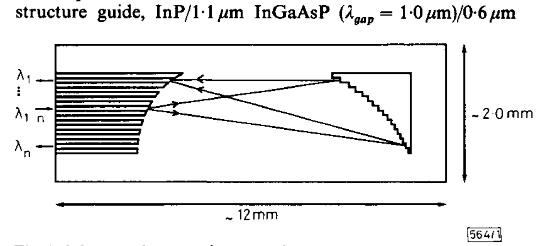

Fig. 1 *Schematic diagram of integrated spectrometer*